

Image Enhancement of Satellite and CCTV using Fuzzy Logic

Jayati Singh, Rahul Dekar
Computer Science and Engineering,
Bansal Institute of Engineering and Technology, Lucknow, India

Abstract: The filtering approach has been proved to be the best when the image is corrupted with salt and pepper noise. The wavelet based approach finds applications in denoising images corrupted with Gaussian noise. Data are transmitted as the high quality digital images in the major fields of communication in all of the modern applications. This paper focused on the work which works on the received image processing before it is used for particular applications. We applied image denoising which involves the manipulation of the DWT coefficients of noisy image data to produce a visually high standard denoised image. This works consist of extensive reviews of the various parametric and non parametric existing denoising algorithms based on statistical estimation approach related to wavelet transforms connected processing approach and contains analytical results of denoising under the effect of various noise at different intensities.

Keywords: PCA, LCA, ICA, Image-denoising

1. Introduction:

A very large portion of digital image processing is devoted to image restoration. This includes research in algorithm development and routine goal oriented image processing. Image restoration is the removal or reduction of degradations that are incurred while the image is being obtained [3]. Degradation comes from blurring as well as noise due to electronic and photometric sources. Blurring is a form of bandwidth reduction of the image caused by the imperfect image formation process such as relative motion between the camera and the original scene or by an optical system that is out of focus [4]. When aerial photographs are produced for remote sensing purposes, blurs are introduced by atmospheric turbulence, aberrations in the optical system and relative motion between camera and ground. In addition to these blurring effects, the recorded image is corrupted by noises too. A noise is introduced in the transmission medium due to a noisy channel, errors during the measurement process and during quantization of the data for digital storage. Each element in the imaging chain such as lenses, film, digitizer, etc. contribute to the degradation. Image denoising is often used in the field of photography or publishing where an image was somehow degraded but needs to be improved before it can be printed. For this type of application we need to know something about the degradation process in order to develop a model for it. When we have a model for the degradation process, the inverse process can be applied to the image to restore it back to the original form. This type of image restoration is often used in space exploration to help eliminate artifacts generated by mechanical jitter in a spacecraft or to compensate for distortion in the optical system of a telescope. Image denoising finds applications in fields such as astronomy where the resolution limitations are severe, in medical imaging where the physical requirements for high quality imaging are

needed for analyzing images of unique events, and in forensic science where potentially useful photographic evidence is sometimes of extremely bad quality [4].

Accurate image modeling, whether done explicitly or implicitly, is a critical component of many image processing tasks. A simple yet effective statistical spatially-adaptive wavelet image model was developed and formed the basis of the state-of-the-art Estimation-Quantization (EQ) compression algorithm. In this work, we develop a closely related model for image wavelet coefficients and apply it to denoising of images corrupted by noise. Our new model significantly reduces the computational burden of an earlier version of our scheme, yet produces comparable results in terms of mean-squared error (MSE) and perceptual image quality. The key ingredient of our new algorithm is the use of simple but efficient spatial adaptation techniques. Our primary goal is to demonstrate the importance of accurate modeling for image denoising problems. In this work, we modify this model for the purpose of image denoising, and demonstrate the benefits of this approach. A related model, that accounts for local dependencies, was independently proposed and its effectiveness was verified by various experimental results. Another related adaptive model was used to perform image denoising via wavelet thresholding using context modeling of the global coefficients histogram. In our work, we take an opposite approach which exploits the local structure of wavelet image coefficients.

2. Related Work:

Recently, the dual-tree complex wavelet transform has been proposed by **Alin Achim et. al. (2005) [15]**, as a novel analysis tool featuring near shift-invariance and improved directional selectivity compared to the standard wavelet transform. Within this framework, we describe a novel technique for removing noise from digital images. We design a bivariate maximum a posteriori estimator, which relies on the family of isotropic α -stable distributions. Using this relatively new statistical model we are able to better capture the heavy-tailed nature of the data as well as the interscale dependencies of wavelet coefficients. We test our algorithm for the Cauchy case, in comparison with several recently published methods. The simulation results show that our proposed technique achieves state-of-the-art performance in terms of root mean squared error.

Aleksandra Pizurica and Wilfried Philips (2006) [9], they develop three novel wavelet domain denoising methods for subband-adaptive, spatially-adaptive and multivalued image denoising. The core of our approach is the estimation of the probability that a given coefficient contains a significant noise-free component, which we call "signal of interest." In this respect, we analyze cases where the probability of signal presence is 1) fixed per subband, 2) conditioned on a local spatial context, and 3) conditioned on information from multiple image bands. All the probabilities are estimated

assuming a generalized Laplacian prior for noise-free subband data and additive white Gaussian noise. The results demonstrate that the new subband-adaptive shrinkage function outperforms Bayesian thresholding approaches in terms of mean-squared error. The spatially adaptive version of the proposed method yields better results than the existing spatially adaptive ones of similar and higher complexity. The performance on color and on multispectral images is superior with respect to recent multiband wavelet thresholding.

This work introduced by **Florian Luisier et. al. (2007) [13]**, a new approach to orthonormal wavelet image denoising. Instead of postulating a statistical model for the wavelet coefficients, we directly parametrize the denoising process as a sum of elementary nonlinear processes with unknown weights. We then minimize an estimate of the mean square error between the clean image and the denoised one. The key point is that we have at our disposal a very accurate, statistically unbiased, MSE estimate—Stein’s unbiased risk estimate—that depends on the noisy image alone, not on the clean one. Like the MSE, this estimate is quadratic in the unknown weights, and its minimization amounts to solving a linear system of equations. The existence of this a priori estimate makes it unnecessary to devise a specific statistical model for the wavelet coefficients. Instead, and contrary to the custom in the literature, these coefficients are not considered random anymore. We describe an interscale orthonormal wavelet thresholding algorithm based on this new approach and show its near-optimal performance—both regarding quality and CPU requirement—by comparing it with the results of three state-of-the-art nonredundant denoising algorithms on a large set of test images. An interesting fallout of this study is the development of a new, group-delay-based, parent–child prediction in a wavelet dyadic tree.

This work presented by **Hossein Rabbani (2009) [17]** a new image denoising algorithm based on the modeling of coefficients in each subband of steerable pyramid employing a Laplacian probability density function (pdf) with local variance. This pdf is able to model the heavy-tailed nature of steerable pyramid coefficients and the empirically observed correlation between the coefficient amplitudes. Within this framework, we describe a novel method for image denoising based on designing both maximum a posteriori (MAP) and minimum mean squared error (MMSE) estimators, which relies on the zero-mean Laplacian random variables with high local correlation. Despite the simplicity of our spatially adaptive denoising method, both in its concern and implementation, our denoising results achieves better performance than several published methods such as Bayes least squared Gaussian scale mixture (BLS-GSM) technique that is a state-of-the-art denoising technique.

A new method based on the curvelet transform is proposed by **Qiang Guo et. al. (2010), [11]** for image denoising. This method exploits a multivariate generalized spherically contoured exponential (GSCE) probability density function to model neighboring curvelet coefficients. Based on the multivariate probability model, which takes account of the dependency between the estimated curvelet coefficients and their neighbors, a multivariate shrinkage function for image denoising is derived by maximum a posteriori (MAP) estimator. Experimental results show that the proposed

method obtains better performance than the existing curvelet-based image denoising method.

3. Methodology:

In the last decade, there has been considerable interest in using multiscale decompositions as a framework to develop algorithms aiming at recovering signals from noisy data. Many of these algorithms have been developed based on Donoho’s pioneering work [1] on soft thresholding. However, wavelet shrinkage techniques have come a long way in recent years due to the better statistical models adopted for the wavelet coefficients. For example, in a number of recent publications [2]–[4], it has been shown that alpha-stable distributions, a family of heavy-tailed densities, are sufficiently flexible and rich to appropriately model wavelet coefficients of images in various applications. On the other hand, algorithms that exploit dependencies between coefficients could achieve better results compared with the ones based on the independence assumption [5]–[8]. In this context, Sendur and Selesnick [7] have developed a maximum a posteriori (MAP) estimator based on a circular-symmetric Laplacian model for a coefficient and its parent.

The wavelet transform is a linear operation. Consequently, after decomposing an image we get, in each of the six oriented subbands and for every two adjacent levels, sets of noisy wavelet coefficients represented as the sum of the transformations of the signal and of the noise

$$y_j = x_j + n_j$$

$$y_{j+1} = x_{j+1} + n_{j+1}$$

where $1 < j < J$ refers to the decomposition level. The above set of equations can be written in vectorial form as

$$y = x + n$$

where $y = (y_j, y_{j+1})$, $x = (x_j, x_{j+1})$, $n = (n_j, n_{j+1})$. The MAP estimator of x given the noisy observation y can be easily derived as being

$$\hat{x}(y) = \operatorname{argmax}_x P_{x|y}(x|y)$$

Using Bayes’ theorem, this equation can be written as

$$\hat{x}(y) = \operatorname{argmax}_x P_n(y - x) P_x(x) = \operatorname{argmax}$$

$$P_n(n) P_x(x)$$

The behavior of this processor incorporates the main property of the ones proposed in [3], and [4] namely that large-amplitude observations are essentially preserved while small-amplitude values are suppressed. In addition, the shrinkage of a coefficient is also conditioned on the value of the corresponding coefficient at the next decomposition level (parent value): The smaller the parent value, the greater the shrinkage [7]. Depending on the noise variance, the “dead zone” of the 2-D shrinkage function (i.e., the circular region where coefficients are heavily shrunk) is more or less extended but the shape of the function remains similar.

3.1 Proposed Work:

The basic idea is to perform wavelet decomposition on the input noisy image, then estimate the noise-free wavelet coefficients by employing a Bayesian estimator, which is developed by using a suitable probability density function (pdf) as a prior for modeling the wavelet coefficients of the image. Finally, the denoised image is reconstructed by performing an inverse wavelet transform.

In contrast to aforementioned conventional parametric model-based approaches, formulate the marginal distribution of wavelet coefficients. Since the proposed non-parametric

wavelet coefficients model automatically adapts to the observed image data, it is expected to yield superior performance to that of the conventional approaches using parametric models that are fixed in advance. Furthermore, a maximum a posteriori (MAP) estimation-based image denoising approach is derived by incorporating the proposed model into a Bayesian inference framework.

A non-parametric statistical model to formulate the distribution of wavelet coefficients, followed by the derivation of the proposed MAP estimation-based image denoising approach. Experimental results are provided to show that the proposed MAP estimation-based image denoising algorithm outperforms the conventional algorithms.

3.1.1 Proposed Image Denoising Approach:

A statistical approach is exploited in this paper to perform image denoising. Given the noisy wavelet coefficient of the noisy image (denoted as y_i , where I is the index), the aim is to recover the noise-free wavelet coefficient (denoted as s_i) via its MAP estimator (denoted as \hat{s}_i) as

$$\hat{s} = arg \max p(s_i | y_i) .$$

According to the Bayes rule, (1) can be rewritten as

$$p(s_i | y_i) = \frac{p(s_i, y_i)}{p(y_i)} \propto p(s_i, y_i) = p(y_i | s_i) p(s_i)$$

The formulation of (2) boils down to the formulations of its two product terms $p(y_i | s_i)$ and $p(s_i)$, respectively. we get

$$p(s_i | y_i) \propto \frac{1}{\sqrt{2\pi}\sigma_n} e^{-\frac{(y_i - s_i)^2}{2\sigma_n^2}} \frac{1}{\sqrt{2\pi}h_j} e^{-\frac{(s_i - y_j)^2}{2h_j^2}}$$

By setting the derivative of (5) to be zero with respect to s_i , we can obtain the MAP estimator of the noise-free coefficient (denoted as \hat{s}_i^j) as

$$\hat{s}_i^j = \frac{\sigma_n^2 y_j + h_j^2 y_i}{\sigma_n^2 + h_j^2}$$

Finally, the estimated noise-free coefficient can be obtained by averaging all MAP estimators, which are obtained by using each component of (4) as the prior image model, respectively; that means

$$\hat{s}_i = \frac{1}{|\Omega_i|} \sum_{y_j \in \Omega_i} \hat{s}_i^j = \frac{1}{|\Omega_i|} \sum_{y_j \in \Omega_i} \frac{\sigma_n^2 y_j + h_j^2 y_i}{\sigma_n^2 + h_j^2} ,$$

where $|\Omega_i|$ represents the number of coefficients in the neighborhood Ω_i .

The noisy images are generated by adding the ground truth image with an additive white Gaussian noise with a zero mean and a standard deviation σ_n , respectively.

The proposed approach first performs a 2-D discrete wavelet decomposition (a five-level decomposition using a Daubechies's wavelet with eight vanishing moments) on a noisy image to get the noisy wavelet coefficients. The wavelet decomposition is implemented via a five-level decomposition using a Daubechies's wavelet with eight vanishing moments. Then, the proposed approach uses (7) to estimate each noise-free coefficient excluding those of the LL subband. Finally, the inverse wavelet transform is applied to obtain the denoised image.

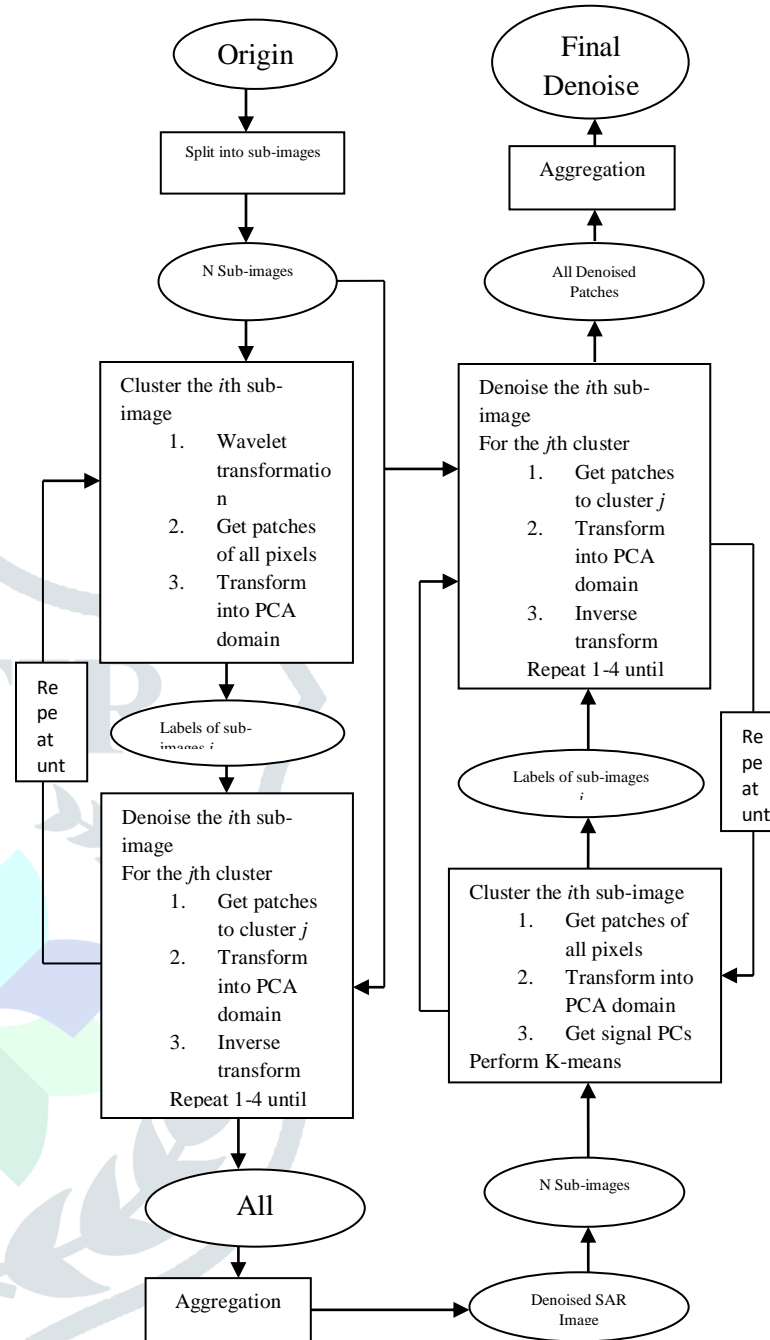


Fig 1. Flow Chart

4. Result and Discussion:

All the collected SAR images are degraded by different levels of Gaussian and speckle noise, respectively. To avoid errors we have taken 15 SAR images and noisy image are produced by adding different noise realizations. All noisy images are processed, and the numerical evaluation is based on the average of the results.

In this work the statistics of peak signal-to-mean-square-error ratio PSNR is used to evaluate these denoising methods. PSNR in case of additive noise is suitable and effective measure of noise in image processing cases.

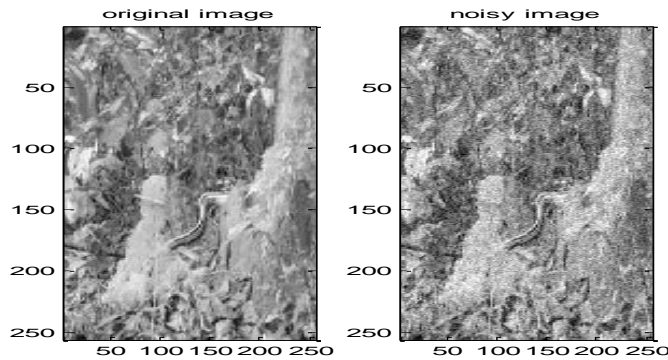


Fig 2 (a): Original SAR image ‘09.jpg’ (left) and noisy image(right).



Figure 2(b): Image block of 64 x 64 from noisy image.

Figure 2(a) shows the original SAR image ‘09.jpg’ and its noisy image obtained by adding Gaussian noise is also shown (figure 2(a) right). Our algorithm extracts 64x64 size block one by one from the noisy image. One of the block of noisy image is shown in figure 1b. This block image is passed through 4 level 2D-DWT wavelet transform operation and we get four approx. The left most i.e first column is approximation blocks (A1,A2,A3,Ad3), then second column represent the horizontal detail (LH1,LH2,LH3 and LH4), third column is vertical details (HL1,HL2,HL3 and HL4) and the last column i.e. fourth represents the diagonal detail coeff.

Each wavelet approx. and detail coefficient matrix of noisy image blocks are passed through one by one through PCA algorithm to obtain the principal components these principal components are labeled in different cluster using K-mean clustering all these matrix are shown in figure 2(d).

The noise components of labeled elements are suppressed from cluster indexed matrix and the reverse PCA and 2d-DWT is applied to reconstruct the denoised image of the stage one as in figure 2(f).

The denoised image obtained in the stage 1 is again taken as reference original image and again whole process is repeated to obtain the new denoised image blocks treating as stage 1 denoised images as original one to find out the noisy clusters in blocks using LMSE values. Hence after end of this stage 2 we obtain the final denoised image shown in figure 2(h). In this figure we can observe the original image (left),noisy image(middle) and finally obtained denoised image on applying stage 2 denoising. We can also observe the PSNR and and noise intensity value given at the top of denoised image and noisy image.

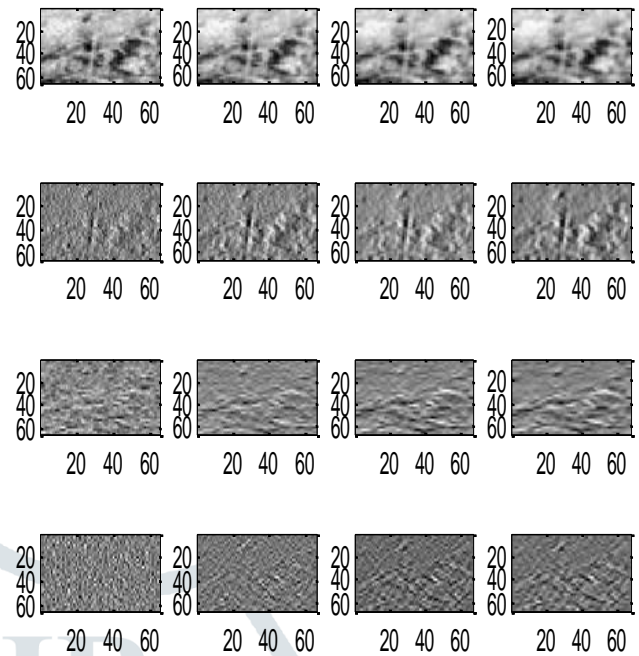


Figure 2(c): Wavelet coeff. Matrix blocks of noisy image block shown in figure (2b).

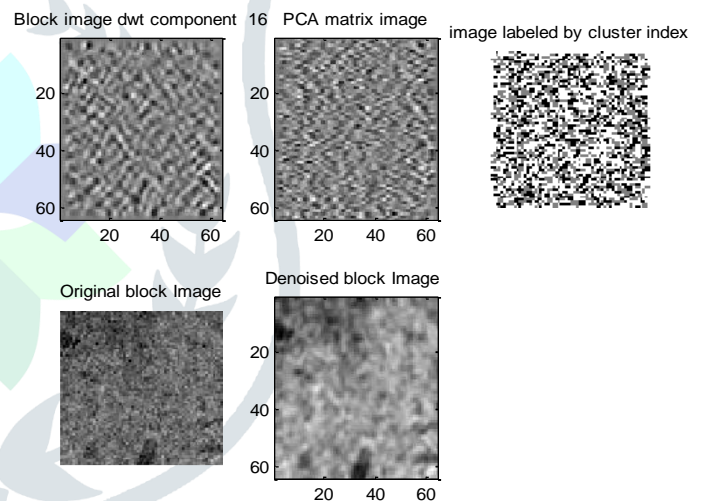


Figure 2(d): Block matrix component image(top left),its PCA matrix (top middle),matrix obtained after cluster indexing (top right).

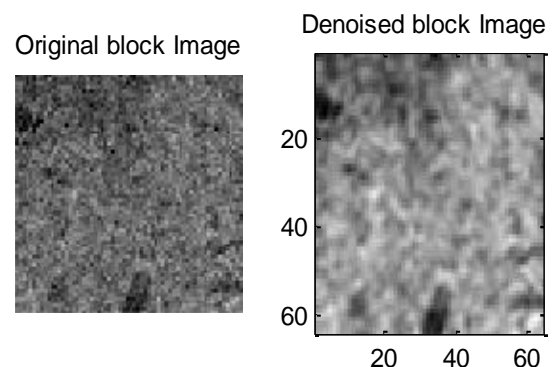


Figure 2(e): Image of arbitrary block taken from Original image (left) and denoised block image obtained in stage 1 of algorithm (right).

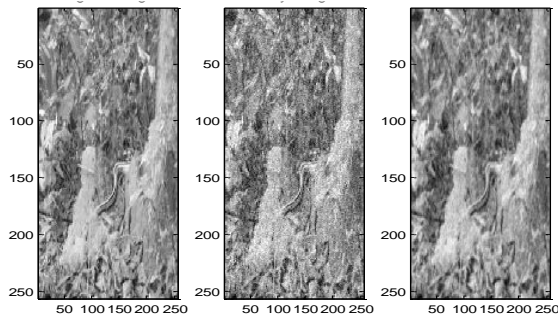


Figure 2(f): Original image (left) , Noisy image (middle) and denoised image of stage1(right)

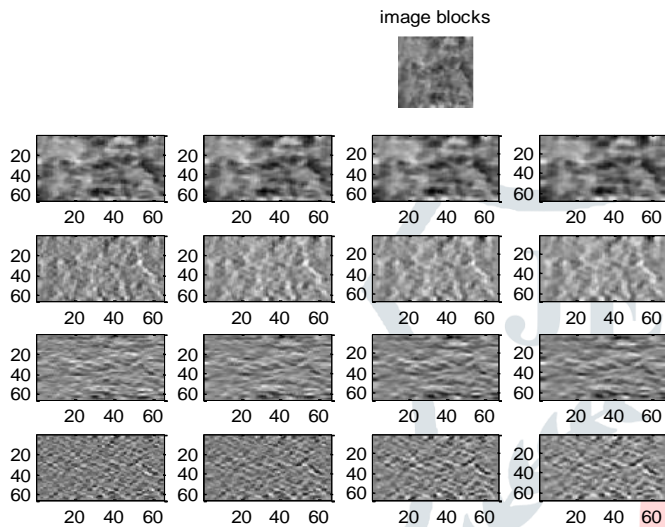


Figure 2(g): Denoised image blocks and its 2d DWT coeff. matrix.

The denoised image obtained in the stage 1 is again taken as reference original image and again whole process is repeated to obtain the new denoised image blocks treating as stage 1 denoised images as original one to find out the noisy clusters in blocks using LMSE values. Hence after end of this stage 2 we obtain the final denoised image shown in figure 2(h). In this figure we can observe the original image (left), noisy image (middle) and finally obtained denoised image on applying stage 2 denoising. We can also observe the PSNR and noise intensity value given at the top of denoised image and noisy image.

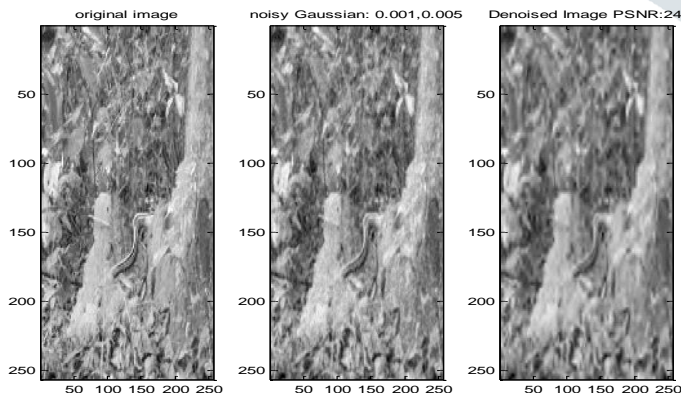


Figure 2(h): Denoised image and its PSNR after denoising.

5. Conclusion:

We have applied our algorithm for analysis of the results of proposed work to various SAR image denoising techniques from the different literature results on standard images. To measure the denoising performance of the improved algorithm we applied the peak signal-to-noise ratio (PSNR). We compared our proposed algorithm to other effective techniques from the different literatures using the standard images. In this work estimation of noise free coefficients is applied to the values of the DWT coefficients of SAR image. We have currently explored the algorithm performance on several images at the effects of different types of noise effect at different noise intensity. We have performed analytical investigation of the results of our proposed algorithm for SAR image denoising techniques and compared results on standard images. In our implementation the bivariate PCA analysis function is applied along with k-mean clustering to the magnitude of the DWT coefficients, which is more shift invariant than the real or imaginary parts. To measure the denoising performance of the improved algorithm we applied the peak signal-to-noise ratio (PSNR). It has been observed that for lossy image processing the PSNR should be in between 25 to 30.

References:

- [1] Z. Cai, T. H. Cheng, C. Lu, and K. R. Subramanian, "Efficient waveletbased image denoising algorithm," *Electron. Lett.*, vol. 37, no. 11, pp. 683–685, May 2001.
- [2] S. Chang, B. Yu, and M. Vetterli, "Adaptive wavelet thresholding for image denoising and compression," *IEEE Trans. Image Processing*, vol. 9, pp. 1532–1546, Sept. 2000.
- [3] Castleman Kenneth R, *Digital Image Processing*, Prentice Hall, New Jersey, 1979.
- [4] Reginald L. Lagendijk, Jan Biemond, *Iterative Identification and Restoration of Images*, Kulwer Academic, Boston, 1991.
- [5] M. S. Crouse, R. D. Nowak, and R. G. Baraniuk, "Wavelet-based signal processing using hidden Markov models," *IEEE Trans. Signal Processing*, vol. 46, pp. 886–902, Apr. 1998.
- [6] D. L. Donoho and I. M. Johnstone, "Ideal spatial adaptation by wavelet shrinkage," *Biometrika*, vol. 81, no. 3, pp. 425–455, 1994.
- [7] L. Kaur, S. Gupta, and R. C. Chauhan, "Image denoising using wavelet thresholding," *Proc. Int. Conf. Computer Vision, Graphics and Image Process.*, pp. 1-4, 2002.
- [8] L. Sendur and I. W. Selesnick, "Bivariate shrinkage with local variance estimation," *IEEE Signal Process. Lett.*, vol. 9, pp. 438-441, 2002.
- [9] A. Pizurica and W. Philips, "Estimating the probability of the presence of a signal of interest in multiresolution single- and multiband image denoising," *IEEE Trans. Image Process.*, vol. 15, pp. 654-665, 2006.
- [10] M. K. Mihcak, I. Kozintsev, K. Ramchandran, and P. Moulin, "Low-complexity image denoising based on statistical modeling of wavelet coefficients," *IEEE Signal Processing Lett.*, vol. 6, pp. 300–303, Dec. 1999.
- [11] Q. Guo and S. Yu, "Image denoising using a multivariate shrinkage function in the curvelet domain," *IEICE Electron. Express*, vol. 7, pp. 126-131, 2010.
- [12] L. Sendur and I. W. Selesnick, "A bivariate shrinkage function for wavelet based denoising," in *IEEE ICASSP*, 2002.

- [13] F. Luisier, T. Blu, and M. Unser, "A new SURE approach to image denoising: Interscale orthonormal wavelet thresholding," *IEEE Trans. Image Process.*, vol. 16, pp. 593-606, 2007.
- [14] I. Prudyus, S. Voloshynovskiy, and A. Synyavskyy, "Wavelet-based MAP image denoising using provably better class of stochastic i.i.d. image models," *Proc. Int. Conf. Telecommun., Modern Satellite, Cable and Broadcasting Service*, pp. 583-586, 2001.
- [15] A. Achim and E. E. Kuruoglu, "Image denoising using bivariate α -stable distributions in the complex wavelet domain," *IEEE Signal Process. Lett.*, vol. 12, pp. 17-20, 2005.
- [16] T. Cai and B.W. Silverman, "Incorporating information on neighboring coefficients into wavelet estimation," *Sankhya*, vol. 63, pp. 127-148, 2001.
- [17] H. Rabbani, "Image denoising in steerable pyramid domain based on a local Laplace prior," *Pattern Recognition*, vol. 42, pp. 2181-2193, 2009.

